Available online at www.sciencedirect.com

ScienceDirect

Ceramics International 39 (2013) 9325–9330

CERAMICS INTERNATIONAL

www.elsevier.com/locate/ceramint

One-step synthesis of CoO anode material for rechargeable lithium-ion batteries

Alok Kumar Rai, Ly Tuan Anh, Jihyeon Gim, Jaekook Kim*

Department of Materials Science and Engineering, Chonnam National University, 300 Yongbong-dong, Bukgu, Gwangju 500-757, Republic of Korea

Received 21 March 2013; received in revised form 2 May 2013; accepted 14 May 2013
Available online 22 May 2013

Abstract

We report a fast method to prepare cobalt oxide (CoO) nanoparticles via urea-assisted auto-combustion synthesis at 300 °C without any post-heat treatment. The structure and morphology were analyzed by synchrotron X-ray diffraction, field-emission scanning electron microscopy, and high-resolution transmission electron microscopy. As-prepared cobalt oxide is cubic, with spherical particle size in the range of 20–30 nm. Electrochemical measurements were performed using the as-prepared powders as the active material for a lithium-ion cell. As an anode for lithium-ion batteries, the nanoparticles electrode exhibited high discharge capacity and good cycling performance with 98% Coulombic efficiency. The nanoparticle electrode delivered a second reversible discharge capacity of 855.47 mA h/g and exhibited ~66% of capacity retention (565.16 mA h/g) after 23 cycles. The enhancement of the electrochemical performance is attributed to the high specific surface area, good electric contact between the particles, and easier lithium ion diffusion.

Keywords: B. X-ray methods; D. Transition metal oxides; E. Batteries

1. Introduction

Designing electrode materials with high lithium storage capacity, rate capability, and long cycling life is still a major challenge for developing high-performance lithium-ion batteries (LIBs). Graphite is currently used as the anode material for commercial LIBs, but its capacity is limited to a theoretical value (372 mA h/g) [1]. More recently, great efforts have been made toward the synthesis of new nanostructured electrode materials to replace graphite anode in LIBs, and to meet the growing demand for use in portable electronic devices and hybrid electric vehicles. In addition, constructing nanostructured electrode materials can produce electrochemical performance that could not be achieved in bulk materials, with benefits of large surface area and short diffusion paths [2–4]. Various new high-performance anode materials have been intensively investigated for next-generation LIBs [5–8]. Transition-metal oxides, such as cobalt oxide, nickel oxide, copper oxide, and iron oxide, have been proposed as promising anode materials because of their high abundance, low cost, environmental benignity, and greater Li^+-ion insertion/extraction capability in excess of 6 Li per formula unit [9,10]. A high reversible capacity about 2 times larger than those of commercial graphite anodes can be achieved [5]. More importantly, the mechanism of Li storage with these transition metal oxides differs from the classical Li^+ ion insertion/deinsertion in graphite anodes or Li alloying processes in alloy electrodes. Among these transition metal oxides, cobalt monoxide (CoO) has attracted special attention due to its higher theoretical Li^+-ion storage capacities (715 mA h/g), and moreover, its electrochemical reaction is completely reversible ($CoO + 2Li^+ + 2e^- \leftrightarrow Co + Li_2O$) [5,11,12]. However, despite this ultra-high capacity, this material suffers from poor conductivity, irreversible capacity loss, and poor cycling stability due to the large volume changes and stresses during the lithium ion insertion/extraction processes, which result in significant capacity fading [12–14].

*Corresponding author. Tel.: +82 62 530 1703; fax: +82 62 530 1699.
E-mail address: jaekook@chonnam.ac.kr (J. Kim).

0272-8842/$ - see front matter © 2013 Elsevier Ltd and Techna Group S.r.l. All rights reserved.
http://dx.doi.org/10.1016/j.ceramint.2013.05.049

The nanostructuring of electrode materials with decreased particles sizes or carbon hybridization has been considered as an effective approach to enhance the structural stability of electrode materials [5,15–17]. Decreasing the particle size can not only alleviate the physical strains, but also improve the reaction kinetics during the lithium ion insertion/deinsertion process. However, despite the appeal of synthesizing nano-size CoO-based anode materials, there are few well-established facile and scalable one-step methods for synthesis [18]. Also, the reported synthesis techniques for such nano-sized electrodes require multiple steps, and are tedious and time-consuming, which significantly hinder the process scale-up.

We present one-step synthesis of CoO nanoparticles by a simple, facile, and inexpensive urea-assisted auto-combustion method without any post-heat treatment. This process produces sub-nanometer-size metal oxide nanoparticles by the self-generated heat of reaction in a very short reaction time. The advantage of using urea is that it can form stable complexes with metal ions to increase solubility and prevent selective precipitation of the metal ions during water removal. In addition, the resultant oxide ash after combustion is generally composed of very fine particles with the desired stoichiometry linked together in a network structure. The present synthesis is very helpful to produce highly crystalline sub-nanometer size particles with distinctive shape and good electrical conductivity between the particles, which exhibit promise for application as an anode material in LIBs.

2. Experimental

2.1. Materials synthesis

CoO powder was prepared by the urea-assisted auto-combustion technique, in which cobalt acetate ($Co(CH_3COO)_2 \cdot 4H_2O$; 98.5%, Junsei), nitric acid (HNO_3; 60.0–62.0%, Daejung), and urea (NH_2CONH_2; 99%, Aldrich) were used as starting materials. Cobalt acetate was converted into its nitrate with the help of dilute nitric acid. An aqueous solution of cobalt nitrate and urea was prepared separately and mixed in appropriate amounts for controlled combustion [19]. The mixed solution was evaporated on a hot plate using a magnetic stirrer at ~300 °C with constant stirring. During evaporation, the homogeneously mixed solution became viscous and turned into a gel, which slowly foamed, swelled and finally burnt on its own. After the burning started at a single point, it propagated forward slowly until the whole sample was fully burnt. The whole process was completed within a few seconds. The nitrates and urea in the combustion mixture act as an oxidizer and fuel, respectively.

According to propellant chemistry, for a stoichiometric redox reaction between a fuel and an oxidizer, the ratio of the net oxidizing valence of the metal nitrate to the net reducing valence of the fuel should be unity. Typical valencies were considered for the most common elements, such as +4 for C, +1 for H, and −2 for O, and the valency for the metallic element was present in the nitrate, such as +2 for Co. A valency of 0 is ascribed to N. For example, the equivalent valency for $Co(NO_3)_2$ is $+2+[0+(-2\times 3)]\times 2=-10$, and that for urea ($NH_2CONH_2$) is $0+2+4+(-2)+0+2=6$. The ideal stoichiometric urea-to-nitrate ratio needed to obtain CoO powders is thus 10:6 or 1.66:1 [20]. The self-generated heat should be sufficient to raise the temperature after ignition. However, it is often insufficient to obtain crystalline powders [21], possibly because the stoichiometric amount of urea is insufficient to attain a sufficiently high peak temperature. Excess urea is thus often used, which may be burned by reaction with the oxygen from air. Therefore, in the present study, the urea-to-nitrate ratio was maintained at 20:6 or 3.32:1 to obtain CoO nanoparticles. The relevant equations are as follows:

$$Co(CH_3COO)_2 \cdot 4H_2O + 2HNO_3 \rightarrow Co(NO_3)_2 + 4H_2O + 2CH_3COOH \quad \text{(i)}$$

$$5Co(NO_3)_2 + \frac{50}{3}NH_2CONH_2 \xrightarrow{\frac{75}{6}O_2} CoO + Co_3O_4 + Co + \frac{65}{3}N_2 + \frac{100}{3}H_2O + \frac{50}{3}CO_2 \quad \text{(ii)}$$

2.2. Materials characterization

The structure of the as-prepared powder was identified by synchrotron X-ray powder diffraction data, which was collected at the 1D high-resolution powder diffraction beamline of the Pohang Accelerator Laboratory, South Korea. Data were collected over an angular 2θ range of 20–80° in steps of 0.01°. The incident X-rays were monochromatized to the wavelength of 1.5476 Å by a double-bounce Si (111) monochromator. The particles morphology and size were observed by field-emission scanning electron microscopy (FE-SEM, S-4700 Hitachi) and high-resolution transmission electron microscopy (HR-TEM, Philips Tecnai F20 at 200 kV). Before obtaining the HR-TEM image, the sample was ultrasonically dispersed in ethanol. A few drops were coated onto a copper grid, and the solvent was subsequently allowed to evaporate in air at room temperature.

2.3. Electrochemical measurements

Electrochemical experiments were carried out using 2032 coin-type cells assembled in an argon-filled glove box. The working electrodes were prepared by mixing the active material (CoO nanoparticles) with super-P and polyvinylidene difluoride at a weight ratio of 80:10:10 in N-methyl-2-pyrrolidone to form a slurry. Then, the resultant slurry was uniformly pasted onto Cu-foil as a current collector with a doctor blade, and then dried at 120 °C in a vacuum oven and pressed between stainless steel twin rollers. Afterward, the foil was punched into circular discs and pressed, and coin cells were assembled with lithium metal as the counter electrode and a Celgard 2400 membrane together with glass fiber as a separator. A solution of 1 M $LiPF_6$ in ethylene carbonate and dimethyl carbonate (1:1 in volume) was used as the electrolyte. The cells were kept in a glove box for 12 h before the

electrochemical measurements. Galvanostatic tests (BTS-2004H, Nagano, Japan) were carried out on the coin cells using a programmable battery tester over the potential range of 0.005–3.0 V vs. Li^+/Li. Cyclic voltammetric (CV) measurement of the electrode was performed on an AUTOLAB potentiostat (PGSTAT302N) with a scan rate of 0.1 mV/s between 0.005 and 3.0 V (vs. Li^+/Li). Electrochemical impedance spectroscopy (EIS) measurements of the electrode were also carried out on the same AUTOLAB potentiostat (PGSTAT302N). The EIS measurements were performed before and after the third cycle of CV measurements. A small AC signal 5 mV in amplitude was used as the perturbation of the system throughout the tests. EIS was used to measure the electronic conductivities of the assembled cell using lithium foil acting as both the counter and reference electrodes.

3. Results and discussion

3.1. Crystal structure and morphology

Fig. 1 shows the synchrotron XRD pattern of the as-prepared CoO powder. All of the diffraction peaks in this pattern are in good agreement with the standard crystallographic data for cubic CoO (JCPDS no. 78-0431, space group *Fm*3*m*). More importantly, the sharp peaks in the XRD pattern suggest a crystalline nature of the as-prepared CoO powder without any post-heat treatment. In addition to the major phase of CoO, small amounts of cubic Co_3O_4 and Co metal peaks are found as impurity phases. The Co element has no ability for lithium-ion storage.

The morphology of the as-prepared CoO powder was studied by FE-SEM, and the recorded image is displayed in Fig. 2(a). The photograph clearly shows that the particles are spherical agglomerates, around ~20–30 nm in size. It is well known that smaller nanoparticles aggregate into secondary particles, which is probably due to their extremely small dimensions and high surface energies. These particles participate in a conversion mechanism that could be detrimental to the cycle performance [22]. To further understand the morphology and structure characteristics of the CoO nanoparticles, HR-TEM was also employed. The HR-TEM picture shown in

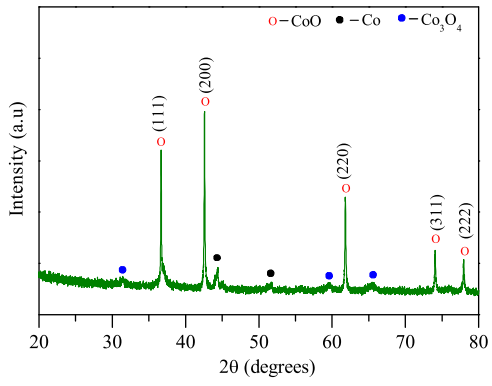

Fig. 1. Synchrotron X-ray powder diffraction pattern of as-prepared CoO nanoparticles.

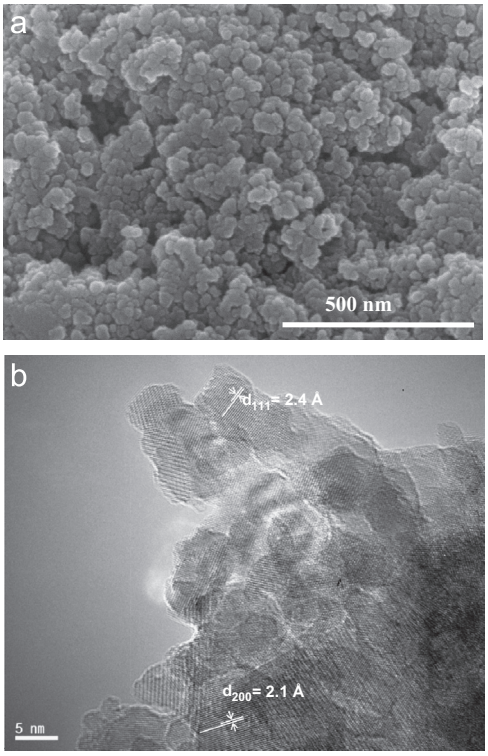

Fig. 2. (a) FE-SEM micrograph and (b) HR-TEM image of as-prepared CoO nanoparticles.

Fig. 2(b) clearly shows interplanar spacings of 2.4 Å and 2.1 Å for the (111) and (200) crystal planes, respectively, which are well matched with the XRD result in Fig. 1. The well-defined lattice fringes reconfirmed that the as-synthesized nanoparticles possessed well-pronounced crystalline structures.

3.2. Electrochemical performance

Fig. 3(a) shows the first and second discharge (lithium insertion) and charge (lithium extraction) curves of the CoO nanoparticles at a constant current density of 0.1 mA/cm^2 with fixed voltages between 0.005 and 3.0 V. The voltage trends are indicative of typical CoO characteristics [5,12]. During the initial discharge, the first voltage that appears at ~1.4 V (24.47 mA h/g) is associated with the lithium storage in CoO. The second flat, long discharge voltage located at ~0.8 V can be ascribed to the conversion reaction between CoO and Li ($CoO + 2Li^+ + 2e^- \leftrightarrow Co + Li_2O$) [23], where a plateau region sets in and continues until a discharge capacity of 830.1 mA h/g is obtained, which corresponds to a consumption of 2.32 mol of Li per mole of CoO. The third slope is observed at a cut-off voltage of 0.005 V, with a total first discharge capacity of 1159.03 mA h/g, corresponding to a consumption of 3.24 mol of Li per mole of CoO, which could be attributed to the interaction of nano-sized Co particles with the electrolyte for the formation of a solid electrolyte interface (SEI) layer [24]. According to the equation, the discharge process should consume 2.0 lithium per CoO, but the experimental value of CoO nanoparticles is 3.24 lithium. The first

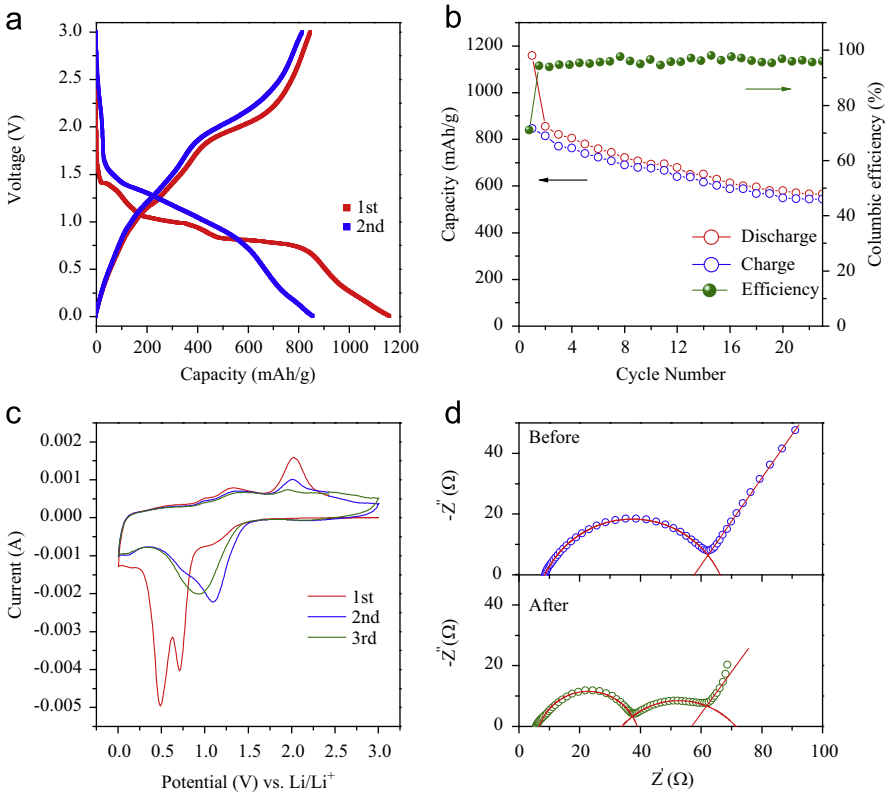

Fig. 3. Electrochemical performances of the as-prepared CoO nanoparticles electrode. (a) Discharge/charge voltage profiles between 0.005 and 3.0 V at the current density of 0.1 mA/cm^2. (b) Capacity retention and Coulombic efficiency plots at the current density of 0.1 mA/cm^2. (c) Cyclic voltammograms at a scan rate of 0.1 mV/S and (d) electrochemical impedance spectroscopy plots of as-prepared CoO nanoparticles before and after CV measurement in the frequency range between 0.01 Hz and 1.0 MHz at room temperature.

charge profile of the CoO nanoparticles shows a strong polarization between 0.0 and 1.85 V followed by a voltage plateau at ~2.0 V. These results could be attributed to the interactions between nano-sized Co and the electrolyte, and the oxidation of nano-sized Co particles with Li_2O, correspondingly [25]. The first charge capacity (Li^+ deinsertion) is 846.13 mA h/g (2.37 mol of Li). The irreversible capacity loss during the first discharge and charge cycle is about 312.9 mA h/g, because of the incomplete decomposition of SEI and Li_2O, and other factors such as the intrinsic nature of the material and kinetic limitations due to current density [26]. After the first discharge, the 0.8 V discharge plateau no longer appears anymore in the second cycle, suggesting a heterogeneous reaction mechanism of lithium insertion and extraction [27,28]. Moreover, the discharge capacity of the CoO nanoparticle electrode decayed to 855.47 mA h/g in the second cycle. Possible reasons for this could be incomplete conversion reaction and irreversible lithium loss due to the formation of an SEI layer [29]. Previous studies have also confirmed that nano-sized cobalt has significant catalytic activity and gives new impetus to the decomposition of Li_2O and the SEI [30]. A reversible charge capacity of 814.47 mA h/g was achieved in the second cycle. The observed capacities are significantly higher than the theoretical capacities of bulk CoO (715 mA h/g) and commercially used graphite anode (372 mA h/g). However, the obtained capacity of the present CoO nanoparticle electrode is comparable to the reported data, which may be attributed to the smaller size, high surface area, and high activity of the nanostructured materials [13,31]. It is also reasonable to suggest that the CoO nanoparticle electrode provides more reaction sites on the surface, and the small diameter provides a short diffusion length for Li^+ ion diffusion, which could enhance the charge transfer and the electrochemical reactions [31].

Fig. 3(b) shows the discharge/charge capacity profile vs. cycle number of the CoO nanoparticle electrode at a constant current density of 0.1 mA/cm^2 for 23 cycles. The specific capacity decreased from 1159.03 mA h/g to 565.16 mA h/g after 23 cycles, which is equivalent to 49% of the initial capacity, and the Coulombic efficiency is maintained at nearly ~98%, indicating good cycleability of the CoO nanoparticle electrode. A possible reason for the good cycling performance of the nanocrystalline CoO electrode is the high degree of crystallization of the material, which results in the reduction of the number of lattice defects, and facilitates the lithium ion insertion and extraction processes. More importantly, the presence of metallic Co greatly increases the electronic conductivity of the electrode materials, and supports the decomposition of Li_2O and the SEI [32]. Remarkably, the observed discharge/charge capacity and cycle number values are not much lower than those reported for CoO nanoparticles, but the synthesis adopted in the present study is cost-effective and simple, and does not require any post-heat treatment, in contrast to previously reported alternatives [25,31].

Fig. 3(c) shows the first three CV curves of the CoO nanoparticle electrode in the range of 0.005–3.0 V with a scan rate of 0.1 mV/s at room temperature. The CV curves are in good agreement with those previously reported for CoO anodes [33]. In the first cycle, two kinds of cathodic peaks appear: a smaller one at 0.71 V and a larger one at 0.48 V, which respectively correspond to the reduction (lithiation) of CoO and the formation of an SEI layer produced below 0.8 V [12,32,34]. In addition, broad peaks located at about 1.31 V during the anodic scan may be attributed to the decomposition of the SEI [35]. The additional anodic peak at 2.02 V can be attributed to the reaction between Co and Li_2O. Compared to the initial cycle, a decrease in peak intensity could be observed with a shift of the lithiation (cathodic) peak from 0.71 V to higher potentials of 1.1 V and 0.93 V in the second and third cycles, respectively. This can be attributed to the newly formed Li_2O, Co products, and reproduced CoO phase, which should be completely amorphous after the first lithiation process [5,32,34]. In general, an amorphous insertion phase will result in the loss of the voltage plateau characteristic for lithium insertion and extraction, in contrast to the initial crystalline CoO [32,34,36,37]. Similar CV results for CoO nanoparticles electrodes were also observed by Wang et al. [13] and Do et al. [38]. The disappearance of the large cathodic peak at 0.48 V in the second cycle indicates that a complete SEI film can be formed on the electrode surface after the first cycle, confirming the almost complete lack of irreversible lithium loss for the SEI film during the following cycles.

An analysis of the impedance response can differentiate between the contributions of Li^+ ion migration through the surface film, the charge transfer through the electrode/electrolyte interface, and the solid-state diffusion of Li^+ ions in the anode [39]. In the impedance spectroscopy, the high-frequency semicircle is attributed to the SEI film and/or contact resistance, while the semicircle in the medium-frequency region is assigned to the charge-transfer impedance at the electrode/electrolyte interface. The inclined line at an approximate angle of 45° to the real axis corresponds to the lithium-diffusion process within the electrodes [40]. Fig. 3(d) presents the EIS spectra obtained before and after the third cycle of CV measurements for the CoO nanoparticle electrode. It is clear that the impedance responses of the cell after the CV measurement differ from that of the fresh cell. The fresh cell shows large impedance with a single depressed semicircle, followed by a Warburg contribution on the low frequency side, which could be due to improper wetting of the electrode by the electrolyte. With the cycling of the cell, due to aging as well as continuous electrochemical interaction, the wetting of the electrode must have improved the electrochemical characteristics of the cell, resulting in diminished charge transfer resistance. Therefore, after CV measurement of the CoO electrode, the shape of the impedance spectra changed completely, and two semicircles were observed. The semicircle in the high-frequency range (SEI film resistance) and the semicircle in the middle frequency range (charge-transfer resistance) were separated. The results of the fitting analysis indicate that the SEI film and charge-transfer resistances were 30.5 Ω and 24.7 Ω, respectively. The latter value obtained is much less than the charge transfer resistance (53.5 Ω) of the fresh cell, which is most probably due to the facile charge transfer at the nano-scale CoO wall/electrolyte interface and the large reduction in the charge-transfer impedance. This reduction of the charge transfer resistance is beneficial to the enhancement of the electron kinetics in the electrode. This agrees well with the results of the electrochemical measurements.

4. Conclusions

Nano-sized CoO powder was synthesized via facile and fast urea-assisted auto-combustion synthesis at 300° C without any post-heat treatment. The as-synthesized CoO powder were characterized using synchrotron XRD, FE-SEM and HR-TEM techniques. The FE-SEM image clearly showed that the particles are spherical agglomerates, around ~20–30 nm in size. The as-synthesized nanoparticles were used as an anode material for Li^+-ion battery, which exhibited an initial discharge capacity of ~1159.03 mA h/g at a current density of 0.1 mA/cm^2. More importantly, 49% of the initial capacity (565.16 mA h/g) could be retained after 23 cycles. The enhanced electrochemical characteristics of the CoO nanoparticle electrodes arise from their relatively high specific surface areas, good electric contact between the particles, and easier lithium ion diffusion. Moreover, the synthesis process is simple and versatile, and could be extended to other metal oxide anode materials used in LIBs applications. Additional intensive research is being carried out to improve the discharge capacity of nanostructured CoO, and will be communicated in the near future.

Acknowledgments

This research was supported by the World Class University (WCU) program through the Korea Science and Engineering Foundation, funded by the Ministry of Education, Science, and Technology (R32-20074). This research was also supported by The Ministry of Knowledge Economy (MKE), Korea, under the Information Technology Research Center (ITRC) support program (NIPA-2013-H0301-13-1009) supervised by the National IT Industry Promotion Agency (NIPA).

References

[1] J.R. Dahn, T. Zheng, Y. Liu, J.S. Xue, Mechanisms for lithium insertion in carbonaceous materials, Science 270 (1995) 590–593.
[2] J. Liu, D. Xue, Hollow nanostructured anode materials for Li-ion batteries, Nanoscale Research Letters 5 (2010) 1525–1534.
[3] J. Liu, H. Xia, D. Xue, L. Lu, Double-shelled nanocapsules of V_2O_5-based composites as high-performance anode and cathode materials for Li ion batteries, Journal of the American Chemical Society 131 (2009) 12086–12087.
[4] J. Liu, D. Xue, Sn-based nanomaterials converted from SnS nanobelts: facile synthesis, characterizations, optical properties and energy storage performances, Electrochimica Acta 56 (2010) 243–250.
[5] P. Poizot, S. Laruelle, S. Grugeon, L. Dupont, J.M. Tarascon, Nano-sized transition-metal oxides as negative-electrode materials for lithium-ion batteries, Nature 407 (2000) 496–499.
[6] G. Derrien, J. Hassoun, S. Panero, B. Scrosati, Nanostructured Sn–C composite as an advanced anode material in high-performance lithium-ion batteries, Advanced Materials 19 (2007) 2336–2340.

[7] J. Xiang, J. Tu, X. Huang, Y. Yang, A comparison of anodically grown CuO nanotube film and Cu_2O film as anodes for lithium ion batteries, Journal of Solid State Electrochemistry 12 (2008) 941–945.
[8] Q. Pan, J. Liu, Facile fabrication of porous NiO films for lithium-ion batteries with high reversibility and rate capability, Journal of Solid State Electrochemistry 13 (2009) 1591–1597.
[9] X. Zhu, Y. Zhu, S. Murali, M.D. Stoller, R.S. Ruoff, Nanostructured reduced graphene oxide/Fe_2O_3 composite as a high-performance anode material for lithium ion batteries, ACS Nano 5 (2011) 3333–3338.
[10] M. Meruganandham, R. Amutha, M. Sathish, T.S. Singh, R.P.S. Suri, M. Sillanpaa, Facile fabrication of hierarchical α-Fe_2O_3: self-assembly and its magnetic and electrochemical properties, Journal of Physical Chemistry C 115 (2011) 18164–18173.
[11] A.S. Aricò, P. Bruce, B. Scrosati, J.M. Tarascon, W.V. Schalkwijk, Nanostructured materials for advanced energy conversion and storage devices, Nature Materials 4 (2005) 366–377.
[12] J.S. Do, C.H. Weng, Preparation and characterization of CoO used as anodic material of lithium battery, Journal of Power Sources 146 (2005) 482–486.
[13] G.X. Wang, Y. Chen, K. Konstantinov, M. Lindsay, H.K. Liu, S.X. Dou, Investigation of cobalt oxides as anode materials for Li-ion batteries, Journal of Power Sources 109 (2002) 142–147.
[14] X.W. Lou, D. Deng, J.Y. Lee, J. Feng, L.A. Archer, Self-supported formation of needlelike Co_3O_4 nanotubes and their application as lithium-ion battery electrodes, Advanced Materials 20 (2008) 258–262.
[15] Y. Xie, C. Wu, Design of nanoarchitectured electrode materials applied in new-generation rechargeable lithium ion batteries, Dalton Transactions 45 (2007) 5235–5240.
[16] Y. Wang, H.J. Zhang, L. Lu, L.P. Stubbs, C.C. Wong, J. Lin, Designed functional systems from peapod-like Co@carbon to Co_3O_4@carbon nanocomposites, ACS Nano 4 (2010) 4753–4761.
[17] X.W. Lou, D. Deng, J.Y. Lee, L.A. Archer, Thermal formation of mesoporous single-crystal Co_3O_4 nano-needles and their lithium storage properties, Journal of Materials Chemistry 18 (2008) 4397–4401.
[18] S. Kundu, M. Jayachandran, Shape-selective synthesis of non-micellar cobalt oxide (CoO) nanomaterials by microwave irradiations, Journal of Nanoparticles Research 15 (2013) 1543–1555.
[19] A.K. Rai, J. Gim, L.T. Anh, J. Kim, Partially reduced Co_3O_4/graphene nanocomposite as an anode material for secondary lithium ion battery, Electrochimica Acta 100 (2013) 63–71.
[20] A. Ringuede, J.A. Labrincha, J.R. Frade, A combustion synthesis method to obtain alternative cermet materials for SOFC anodes, Solid State Ionics 141–142 (2001) 549–557.
[21] A. Ringuede, J.R. Frade, J.A. Labrincha, Combustion synthesis of zirconia-based cermet powders, Ionics 6 (2000) 273–278.
[22] A.K. Rai, J. Gim, S.W. Kang, V. Mathew, L.T. Anh, J. Kang, J. Song, B.J. Paul, J. Kim, Improved electrochemical performance of $Li_4Ti_5O_{12}$ with a variable amount of graphene as a conductive agent for rechargeable lithium-ion batteries by solvothermal method, Materials Chemistry and Physics 136 (2012) 1044–1051.
[23] J.S. Do, R.F. Dai, Cobalt oxide thin film prepared by an electrochemical route for Li-ion battery, Journal of Power Sources 189 (2009) 204–210.
[24] F.D. Wu, Y. Wang, Self-assembled echinus-like nanostructures of mesoporous CoO nanorod@CNT for lithium-ion batteries, Journal of Materials Chemistry 21 (2011) 6636–6641.
[25] C.H. Chen, B.J. Hwang, J.S. Do, J.H. Wengd, M. Venkateswarlu, M.Y. Cheng, R. Santhanam, K. Ragavendran, J.F. Lee, J.M. Chen, D.G. Liu, An understanding of anomalous capacity of nano-sized CoO anode materials for advanced Li-ion battery, Electrochemistry Communications 12 (2010) 496–498.
[26] M.V. Reddy, T. Yu, C.H. Sow, Z.X. Shen, C.T. Lim, G.V. Subba Rao, B.V.R. Chowdari, α-Fe_2O_3 nanoflakes as an anode material for Li-ion batteries, Advanced Functional Materials 17 (2007) 2792–2799.
[27] S. Grugeon, S. Laruelle, L. Dupont, J.M. Tarascon, An update on the reactivity of nanoparticles Co-based compounds towards Li, Solid State Sciences 5 (2003) 895–904.
[28] P. Poizot, S. Laruelle, S. Grugeon, J.M. Tarascon, Rationalization of the low-potential reactivity of 3d-metal-based inorganic compounds toward Li, Journal of the Electrochemical Society 149 (2002) A1212–A1217.
[29] W. Yao, J. Yang, J. Wang, Y. Nuli, Multilayered cobalt oxide platelets for negative electrode material of a lithium-ion battery, Journal of the Electrochemical Society 155 (2008) A903–A908.
[30] R. Malini, U. Uma, T. Sheela, M. Ganesan, N.G. Renganathan, Conversion reactions: a new pathway to realise energy in lithium-ion battery-review, Ionics 15 (2009) 301–307.
[31] H. Qiao, L. Xiao, Z. Zheng, H. Liu, F. Jia, L. Zhang, One-pot synthesis of CoO/C hybrid microspheres as anode materials for lithium-ion batteries, Journal of Power Sources 185 (2008) 486–491.
[32] L. Zhang, P. Hu, X. Zhao, R. Tian, R. Zou, D. Xia, Controllable synthesis of core–shell Co@CoO nanocomposites with a superior performance as an anode material for lithium-ion batteries, Journal of Materials Chemistry 21 (2011) 18279–18283.
[33] W. Yao, J. Chen, H. Cheng, Platelike CoO/carbon nanofiber composite electrode with improved electrochemical performance for lithium ion batteries, Journal of Solid State Electrochemistry 15 (2011) 183–188.
[34] S. Laruelle, S. Grugeon, P. Poizot, M. Dollé, L. Dupont, J.M. Tarascon, On the origin of the extra electrochemical capacity displayed by MO/Li cells at low potential, Journal of the Electrochemical Society 149 (2002) A627–A634.
[35] F. Li, Q.Q. Zou, Y.Y. Xia, CoO-loaded graphitable carbon hollow spheres as anode materials for lithium-ion battery, Journal of Power Sources 177 (2008) 546–552.
[36] M. Dollé, P. Poizot, L. Dupont, J.M. Tarascon, Experimental evidence for electrolyte involvement in the reversible reactivity of CoO toward compounds at low potential, Electrochemical Solid-State Letters 5 (2002) A18–A21.
[37] R. Dedryvère, S. Laruelle, S. Grugeon, P. Poizot, D. Gonbeau, J.M. Tarascon, Contribution of X-ray photoelectron spectroscopy to the study of the electrochemical reactivity of CoO toward lithium, Chemistry of Materials 16 (2004) 1056–1061.
[38] J.S. Do, C.H. Weng, Electrochemical and charge/discharge properties of the synthesized cobalt oxide as anode material in Li-ion batteries, Journal of Power Sources 159 (2006) 323–327.
[39] D. Aurbach, M.D. Levi, K. Gamulski, B. Markovsky, G. Salitra, E. Levi, U. Heider, L. Heider, R. Oesten, Capacity fading of $Li_xMn_2O_4$ spinel electrodes studied by XRD and electroanalytical techniques, Journal of Power Sources 81–82 (1999) 472–479.
[40] S. Yang, H. Song, X. Chen, Electrochemical performance of expanded mesocarbon microbeads as anode material for lithium-ion batteries, Electrochemistry Communications 8 (2006) 137–142.